

# Simple algebraic method to study the effects of hydrostatic pressure on the fundamental parameters of a Schottky barrier of metal/*n*-GaAs

O. Oubram

*Facultad de Ciencias Químicas e Ingeniería, Universidad Autónoma del Estado de Morelos,  
Av. Universidad 1001, Col. Chamilpa, 62209 Cuernavaca, Morelos, México.*

L.M. Gaggero-Sager

*Facultad de Ciencias, Universidad Autónoma del Estado de Morelos,  
Av. Universidad 1001, Col. Chamilpa Cuernavaca, Morelos 62210, México.*

I. Rodríguez-Vargas

*Unidad Académica de Física, Universidad Autónoma de Zacatecas,  
Calzada Solidaridad Esquina con Paseo la Bufa S/N, Zacatecas, Zac., 98060, México,  
e-mail: isaac@fisica.uaz.edu.mx*

Received 10 February 2015; accepted 18 May 2015

The effects of hydrostatic pressure on the fundamental parameters of a Schottky barrier diode of metal/*n*-GaAs are studied using a simple algebraic method. The method relies on the dependence of the parameters of the semiconductor (effective mass, dielectric constant and band gap) with the hydrostatic pressure. We obtain simple expressions for the Schottky Barrier Height, Background Density and Differential Capacity that account of the hydrostatic pressure readily. In particular, the Schottky Barrier Height expression agrees qualitatively with the experimental results available. The Differential Capacity expression depends directly on the effective mass, opening the possibility of determined the effective mass through capacitance measurements. Due to its simplicity the algebraic method could be useful in the design of devices that exploit hydrostatic pressure effects.

*Keywords:* Hydrostatic pressure; Schottky barrier height; differential capacitance; algebraic method.

PACS: 73.30+y; 73.40.Ns; 74.62.F

## 1. Introduction

The investigation of metal-semiconductor (MS) contacts, commonly known as Schottky barrier diodes (SBDs), is a very important topic from both theoretical and practical research. Metal semiconductor structures are important tools used for the characterization of new semiconductors and the fabrication of these structures plays a crucial role in the construction of useful technological devices [1-10]. In addition to that, Schottky contacts on group III-V semiconductors have been widely applied in high speed electronic and optoelectronic devices such as diodes, field-effect transistors, high electronic mobility transistors, solar cells, etc. [11-14].

Because of the technological importance of SBDs a full understanding of the nature of the electrical characteristic is of great interest [15]. However, despite of years of extensive research and widespread use of Schottky contacts in device technology, the fundamental mechanism responsible for the formation of the Schottky barrier is still not fully understood [15]. The complexity of SBDs comes from the dependence of the Schottky barrier on the atomic structure of the MS interface. Due to the particularities of each MS interface the lack of general expressions, based on a quantum-mechanical description, of the Schottky barrier parameters is still present [15]. Within this context, simple theories that provide information of the Schottky barrier parameters are still valuable and could be useful in the design of technologi-

cal applications based on Schottky barriers. Among these theories, one that has been widely used is the thermionic emission theory [16]. In this theory, the Fermi-level pinning is of paramount importance, since it determines the Schottky Barrier Height (SBH). Different models for the Fermi-level pinning have been proposed, among the most popular ones, we can find the metal-induced gap states (MIGS) [17-19] and the defect model [20-22].

Within this context, the Schottky barrier under hydrostatic pressure (HP) is not the exception. Even more, if we consider the relevance of pressure effects as a mechanism to modulate the optoelectronic and transport properties of micro-mechanical devices, as well as a natural condition for devices working in extreme environments, see for instance [23-26]. So, different models have been implemented in order to explain the observed variations of the SBH with the hydrostatic pressure [27-43]. Despite the particularities that we can find in these reports, in general, under pressure, both the semiconductor and the MS interface are affected. In particular, it is reported that the rectifying properties of SBDs are improved under hydrostatic pressure. Besides, a linear increase of the SBH with the HP is observed. An important parameter that helps to discern if the changes in the semiconductor or in the semiconductor and MS interface are important in the determination of the SBH is the ideality factor [16]. The ideality factor is a parameter that accounts how perfect or ideal a junction is, or equivalently how much a SBD de-

viates from the ideal behavior (Diode Law) due to interfacial inhomogeneities. In particular, if the ideality factor is much greater than 1, then the changes in the MS interface become important. Specifically interface states, series resistance and a interfacial layer can come into play. To this respect, it has been shown that the increase of the SBH and the improvement of the rectifying properties of SBDs obey a decrease in the interface state density. Last but not least to mention, it is that irrespective if the changes in the MS interface are important or not, the SBH variation comes from the changes suffered by the effective band gap of the system, since at the end the Fermi level pinning is what determines the SBH.

Here, we show that using a simple algebraic method it is possible to obtain readily the Schottky barrier parameters as a function of the hydrostatic pressure for metal/*n*-GaAs. The algebraic method is based on the assumption that practically all relevant parameters of the semiconductor vary with HP. Specifically, the variation of the band-gap and the dielectric constant with pressure have a direct impact on the effective Bohr radius and effective Rydberg. We determined algebraically the SBH, screening distance, background impurity density, potential profile and Differential Capacitance of metal/*n*-GaAs for different values of the hydrostatic pressure and temperature. In the case of the SBH and the inverse square of the Differential Capacitance we have found an increasing and decreasing behaviour with respect to HP, which agrees quite well from a qualitative stand point as compared to the experimental data available. Additionally, the algebraic formalism provides a direct relation between the Differential Capacitance and the effective mass for metal/*n*-GaAs under pressure, opening the possibility to determine the effective mass through Capacitance measurements.

## 2. Theory and Results

### 2.1. Schottky Barrier Height

As we already mentioned, there are different models to deal with hydrostatic pressure effects on SBDs. Here, we consider a quite different approach. The basic idea of the analysis is to suppose that all the parameters of the systems can be written in effective atomic units [44,45]: effective Bohr radius and effective Rydberg. Moreover, as the hydrostatic pressure modifies the interatomic distance of crystals [46,47], parameters such as the energy band-gap, the dielectric constant and the effective mass change as well [48]. Then, as the effective units depend on these parameters, the effects of the hydrostatic pressure can be incorporated via the effective atomic units. Explicitly, we can write the effective Bohr radius as,

$$a_0^*(P, T) = \frac{\varepsilon_r(P, T) \hbar^2}{m^*(P, T) e^2}, \quad (1)$$

and the effective Rydberg as

$$R_y^*(P, T) = \frac{e^2}{2\varepsilon_r(P, T) a_0^*(P, T)}, \quad (2)$$

where the pressure and temperature dependent effective mass is given by [49,50],

$$m^*(P, T) = \left[ 1 + \frac{2 \times 7510}{E_{\text{gap}}(P, T)} + \frac{7510}{E_{\text{gap}}(P, T) + 341} \right]^{-1} m_0, \quad (3)$$

here  $m_0$  is the free electron mass and  $E_{\text{gap}}(P, T)$  is the pressure-temperature dependent gap for GaAs at the  $\Gamma$  point in units of meV, this parameter is given by [49],

$$E_{\text{gap}}(P, T) = E_1 + \beta P + \alpha T^2 / (T + 204), \quad (4)$$

where in the  $\Gamma$  point  $E_1(P) = 1519$  meV,  $\beta = 10.7$  meV/kbar and  $\alpha = -0.5405$  meV/K. The pressure-temperature dependent dielectric constant comes as [49]

$$\varepsilon_r(P, T) = \varepsilon_a e^{\alpha_1 T + \alpha_2 P}. \quad (5)$$

In Eq. (5) for  $T \leq 200$  K ( $T > 200$  K) we use the following parameters  $\varepsilon_a = 12.65$  ( $= 12.29$ ),  $\alpha_1 = 9.4 \times 10^{-5} \text{ K}^{-1}$  ( $= 20.4 \times 10^{-5} \text{ K}^{-1}$ ) and  $\alpha_2 = -1.67 \times 10^{-3} \text{ kbar}^{-1}$  ( $= -1.73 \times 10^{-3} \text{ kbar}^{-1}$ ).

From Eqs. (3) and (5) we can notice that as the hydrostatic pressure increases the effective mass and the dielectric constant increases and decreases, respectively. Likewise, we can see that the Bohr radius and the effective Rydberg reduces and increases as the pressure increases. Taking into account these modifications, we proceed by writing the expression for the height of the Schottky diode in atomic units as a function of the pressure for the special case of a metal/*n*-GaAs system. By supposing that we are in the low pressure limit ( $P < 6$  kbar), the SBH can be written as,

$$e\Phi(P, T) = e\Phi^* R_y^*(P, T), \quad (6)$$

where  $e\Phi(P, T)$  is the height of the barriers as a function of the hydrostatic pressure  $P$  and temperature  $T$ ,  $e\Phi^*$  is the height of the barrier without pressure effects and  $R_y^*(P, T)$  is the pressure-temperature dependent effective Rydberg. Therefore,  $e\Phi(P, T)$  can be written in effective atomic units as

$$e\Phi(P, T) = e\Phi^* R_y \frac{m^*(P, T)}{\varepsilon_r^2(P, T)}, \quad (7)$$

where  $R_y$  is the effective Rydberg without pressure. Let us now define the relative theoretical Schottky barrier as follows

$$e\Phi_{\text{rel}}^{\text{theo}}(P, T) = \frac{e\Phi(P, T)}{e\Phi(P=0, T)}, \quad (8)$$

after some straightforward algebra  $e\Phi_{\text{rel}}^{\text{theo}}(P, T)$  can be expressed in the following way

$$e\Phi_{\text{rel}}^{\text{theo}}(P, T) = \frac{m^*(P, T) \varepsilon_r^2(P=0, T)}{\varepsilon_r^2(P, T) m^*(P=0, T)}. \quad (9)$$

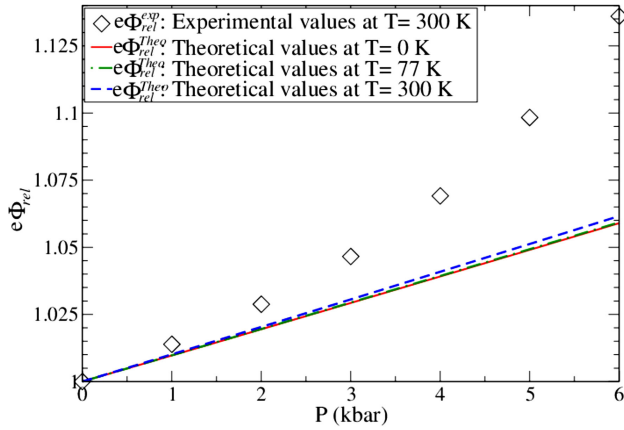


FIGURE 1. (Color online) Evolution of the relative SBH in Au/n-GaAs as a function of hydrostatic pressure. The curves from top to bottom correspond to the relative experimental SBH for  $T = 300$  K, the relative theoretical SBH when  $T = 300$  K, the relative theoretical SBH for  $T = 77$  K and the relative theoretical SBH for  $T = 0$  K.

Substituting the effective mass Eq. (3) and dielectric constant Eq. (5) and by using Taylor series expansion up to fourth order in the pressure, we obtain for  $T = 0$  K,

$$e\Phi_{\text{rel}}^{\text{theo}}(P) = 1 + 0.95 \times 10^{-2}P + 0.232 \times 10^{-4}P^2 + 0.34 \times 10^{-7}P^3 + \theta(P^4), \quad (10)$$

and for  $T = 300$  K,

$$e\Phi_{\text{rel}}^{\text{theo}}(P) = 1 + 0.999 \times 10^{-2}P + 6.4 \times 10^{-4}P^2 + 0.363 \times 10^{-7}P^3 + \theta(P^4). \quad (11)$$

These two last expressions are the ones we are going to use to compare the relative experimental height of the Schottky barrier. The experimental expression for the SBH as a function of the hydrostatic pressure for Au/n-GaAs is [41],

$$e\Phi^{\text{exp}}(P) = e\Phi^{\text{exp}}(P=0) + \alpha P + \beta P^2 + \gamma P^3. \quad (12)$$

In this equation we have considered  $T = 300$  K, so  $\alpha = 11.21$  meV/kbar,  $\beta = -0.345$  meV/kbar<sup>2</sup> and  $\gamma = 0.25$  meV/kbar<sup>3</sup>. In order to compare with Eq. (11), we define the relative experimental height of the Schottky diode as,

$$e\Phi_{\text{rel}}^{\text{exp}}(P) = \frac{e\Phi^{\text{exp}}(P)}{e\Phi^{\text{exp}}(0)}, \quad (13)$$

thus, by substituting Eq. (12) into Eq. (13), we obtain

$$e\Phi_{\text{rel}}^{\text{exp}}(P) = 1 + 1.40 \times 10^{-2}P - 43 \times 10^{-5}P^2 + 3.125 \times 10^{-4}P^3 + \theta(P^4). \quad (14)$$

Figure 1 shows the results of  $\Phi_{\text{rel}}^{\text{theo}}(P)$  for  $T = 0$  K,  $T = 77$  K and  $T = 300$  K and the result of  $e\Phi_{\text{rel}}^{\text{exp}}(P)$  for  $T = 300$  K. Some relevant aspects that should be pointed out are the following:  $\Phi_{\text{rel}}^{\text{theo}}(P)$  and  $\Phi_{\text{rel}}^{\text{exp}}(P)$  have the same behavior for pressures below 4 kbar, whereas the difference

between experimental and theoretical model is under 7 percent for pressures in the range of  $4 \text{ kbar} < P < 6 \text{ kbar}$ . We can also see that the SBH decreases as the temperature decreases as well, as claimed by Mangal and Banerji [13]. So, despite the simplicity of our model we can see that it agrees qualitatively with the experimental results, and quantitatively in a specific range of pressures.

## 2.2. Potential profile

In this section we will analyze the SBD when in addition to the pressure, there is also a contact voltage  $V_c$ . If we apply a difference of potential of 500 meV in the metal-semiconductor contact, we can study the profile of the potential, the penetration distance of the electric field (Debye distance) and the background density. Here it is important to mention that we are considering a potential of 500 meV, because it is a typical value in Schottky barriers in GaAs. Indeed, in principle, we can apply any potential, however if the potential is too high the one band model that we are using is not longer appropriate. Besides, Schottky Barrier Diodes come with a low-dimensional system, such as for example a quantum well, so if the potential is too high the quantum well system will be totally depleted and consequently its characteristics will be inconsequential for the device. Therefore, as a general criterion we can say that the potential can not surpass the bandgap of the hot material, in our case the bandgap of GaAs, which is approximately equal to 1400 meV.

The model for describing the metal/n-GaAs profile potential is [16],

$$V(z) = \frac{2\pi e^2}{\epsilon_r} N_d (z - L)^2, \quad (15)$$

where  $N_d$  is the background impurity density,  $\epsilon_r$  is the electric permittivity constant of GaAs and  $L$  is the screening distance of the electric field given by

$$L = \sqrt{\frac{\epsilon_r V_c}{2\pi e^2 N_d}}, \quad (16)$$

here  $V_c$  is the contact voltage. Following the spirit of this paper, when we apply the hydrostatic pressure all the physical parameters of the system change, therefore the potential profile would have the following form

$$V(z, P) = \frac{2\pi e^2}{\epsilon_r(P)} N_d(P) (z(P) - L(P))^2. \quad (17)$$

Writing the potential profile, the Debye distance and background distance in atomic units we get

$$V(z, P) = V^* R_y^*(P), \quad (18)$$

$$L(P) = L^* a_0^*(P), \quad (19)$$

$$N_d(P) = N_d^* \frac{1}{a_0^{*3}(P)}. \quad (20)$$

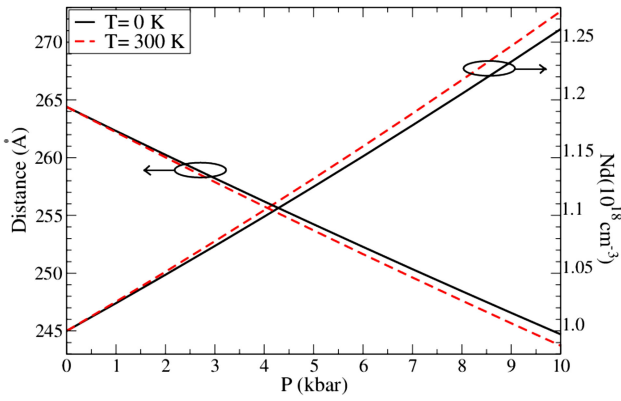


FIGURE 2. (Color online) (Left to right) Screening distance of the electric field and (Right to left) background impurity density as a function of the applied hydrostatic pressure for two different values of the temperature. Solid-black (dashed-red) curve corresponds to  $T=0$  K ( $T=300$  K).

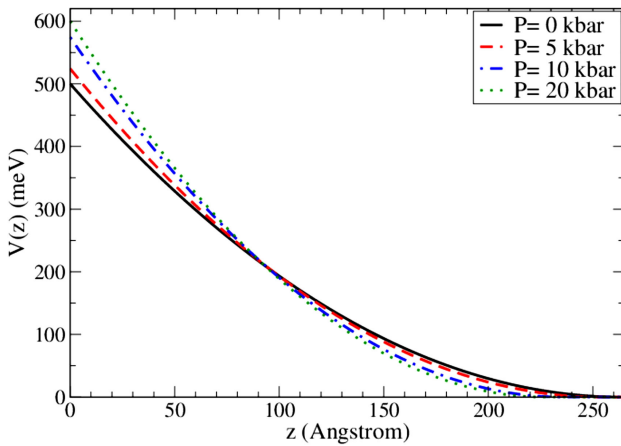


FIGURE 3. (Color online) Potential profile for metal-semiconductor in GaAs for four different values of hydrostatic pressure. The solid-black, dashed-red, dashed-dotted-blue and dotted-green curves correspond to pressures of 0, 5, 10 and 20 kbar, respectively.

From these expressions we can readily see that the background density increases linearly with pressure and the screening distance decreases when the hydrostatic pressure is applied, see Fig. 2. In Fig. 3 we can see a crossover in  $V(z, P)$  about  $100 \text{ \AA}$ , specifically we can notice that for values below  $100 \text{ \AA}$  the potential increases as the pressure increases as well, while for values above  $100 \text{ \AA}$  the potential diminishes as the pressure rises.

### 2.3. Analytical Differential Capacity

Other of the principal characteristics of the metal-semiconductor system is the Differential Capacitance. As we have shown through this paper when hydrostatic pressure is applied to the system the parameters of it change. Within this context, the Differential Capacitance is not the exception, since it depends on the mentioned parameters. The Differential Capacitance can be defined as [16]

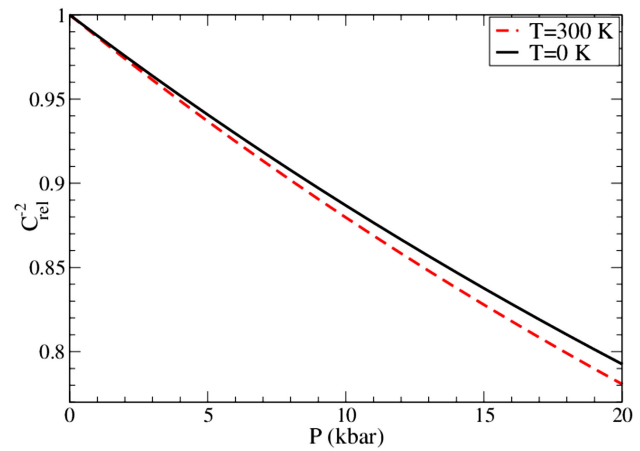


FIGURE 4. (Color online) Reverse bias  $C_{\text{rel}}^{-2}$  characteristics for the metal/n-GaAs Schottky barrier diode as a function of hydrostatic pressure in the range of 0 – 20 kbar for  $T=0$  K (solid-black) and  $T=300$  K (dashed-red).

$$C = \frac{\partial Q_d}{\partial e\Phi}, \quad (21)$$

with  $Q_d = -eN_dL$  the charge of the donors in the depletion zone,  $N_d$  the impurity background density,  $L$  the width of the depletion layer and in this case also the penetration distance of the electric field inside the semiconductor, and  $e\Phi$  the height of the Schottky barrier. Thus we can write

$$C = -eN_d \frac{\partial L}{\partial e\Phi}, \quad (22)$$

or

$$C(P) = -eN_d(P) \frac{\partial L(P)}{\partial e\Phi(P)}. \quad (23)$$

Inserting Eqs. (6), (19) and (20) in this expression one gets

$$C(P) = -eN_d^* \frac{\partial L^*}{\partial e\Phi^*} \frac{1}{R_y(P) a_0^{*2}(P)}, \quad (24)$$

in this equation the term

$$-eN_d^* \frac{\partial L^*}{\partial e\Phi^*}, \quad (25)$$

is independent of pressure effects. To analyze Eq. (24) let us define the relative differential capacitance

$$C_{\text{rel}} = \frac{C(P)}{C(0)}, \quad (26)$$

and using the expressions for  $R_y(P)$  and  $a_0^*(P)$ , Eqs. (1) and (2), the relative differential capacitance is going to have the following form

$$C_{\text{rel}} = \frac{m^*(P)}{m^*(0)}. \quad (27)$$

Usually the differential capacitance is reported experimentally as  $C_{\text{rel}}^2$ . Thus, we have

$$C_{\text{rel}}^2 = \frac{m^{*2}(P)}{m^{*2}(0)}. \quad (28)$$

From this expression we obtain the results shown in Fig. 4, for different temperatures. We can see that  $C_{\text{rel}}^{-2}$  has a downward and linear adjustment. This almost linear behaviour give us a valuable tool because it allows to measure the variation of the effective mass as a function of pressure. Another observation to emphasize is the fact that Eq. (28) is independent of the applied potential  $V_c$ , as was shown by G. Çankaya for Cd/p-GaTe [31].

### 3. Conclusions

In summary, we have implemented a simple algebraic method to study the variation of the fundamental parameters of SBDs when hydrostatic pressure is applied. This method allows us to obtain simple expressions for the SBH, screening distance, background impurity density, potential profile and differen-

tial capacitance. Despite the simplicity of the method, the results agree qualitatively, and in some range of pressures quantitatively, with the experimental data available. Additionally, it provides an expression for the differential capacitance, that depends directly of the effective mass, opening the possibility of know the effective mass through capacitance measurements. Due to its simplicity the algebraic method could provide useful information for the design of devices that work under extreme conditions of pressure and temperature such as high power laser diodes.

### Acknowledgments

O.O. acknowledges the financial support of PROMEP through grant NPTC-2013.

1. D.M. Moss, A.V. Akimov, B.A. Glavin, M. Henini, and A.J. Kent, *Phys. Rev. Lett.* **106** (2011) 066602.
2. H. Saito, Y. Mineno, S. Yuasa, and K. Ando, *J. Appl. Phys.* **109** (2011) 07C701.
3. S. Averine, Y.C. Chan, and Y.L. Lam, *Appl. Phys. Lett.* **77** (2000) 274.
4. S.Y. Cheng, *Mater. Chem. Phys.* **78** (2003) 525.
5. J.Y. Park and G.A. Somorjai, *J. Vac. Sci. Technol. B* **24** (2006) 1967.
6. O.E. Tereshchenko *et al.*, *J. Appl. Phys.* **109** (2011) 113708.
7. S.J. Young, *IEEE Sens. J.* **11** (2011) 1129.
8. S. Tripathi and S. Jit, *J. Appl. Phys.* **109** (2011) 053102.
9. Y. Xie, H. Huang, W. Yang, and Z. Wu, *J. Appl. Phys.* **109** (2011) 023114.
10. D. Li, X. Sun, H. Song, Z. Li, Y. Chen, G. Miao, and H. Jiang, *Appl. Phys. Lett.* **98** (2011) 011108.
11. G.Y. Robinson, *In Physics and Chemistry of III-V Compound Semiconductor Interfaces*, edited by C.W. Wilmsen-Plenum, (New York 1985).
12. R. Zucca and E.J. Wood, *J. Appl. Phys.* **46** (1975) 3.
13. S. Mangal and P. Banerji, *J. Appl. Phys.* **105** (2009) 083709.
14. A. Keffous, M. Zitouni, Y. Belkacem, H. Menari, and W. Chergui, *Appl. Surf. Sci.* **199** (2002) 22.
15. R.T. Tung, *Appl. Phys. Rev.* **1** (2014) 011304.
16. E.H. Rhoderick, R.H. Williams, *Metal-semiconductor Contacts*, Clarendon Press, (Oxford 1988).
17. C. Tejedor, F. Flores and E. Louis, *J. Phys. C: Solid State Phys.* **10** (1977) 2163.
18. J. Tersoff, *Phys. Rev. B* **30** (1984) 4874.
19. J. Tersoff, *Phys. Rev. B* **32** (1985) 6968.
20. W. E. Spicer, I. Lindau, P. Skeath, C. Su, and P. Chye, *J. Vac. Sci. Technol.* **17** (1979) 1019.
21. W. Walukiewicz, *J. Vac. Sci. Technol. B* **5** (1987) 1062.
22. W. E. Spicer *et al.*, *J. Vac. Sci. Technol. B* **6** (1988) 1245.
23. F. Dybala, A. Bercha, M. Klimczak, B. Piechal, Y. Ivonyak, W.A. Trzeciakowski, *physica status solidi (b)* **250** (2013) 703.
24. A. Bercha *et al.*, *physica status solidi (b)* **250** (2013) 769.
25. A. Patane and N. Balkan, *Semiconductor Research: Experimental Techniques*, (Springer Series in Materials Sciences, 2012).
26. E.P. O'Reilly, G. Jones, M. Silver and A.R. Adams, *physica status solidi (b)* **198** (1996) 363.
27. S. Fiat and G. Cankaya, *Mat. Sci. Semicon. Proc.* **15** (2012) 461.
28. N. Ucar, A.F. Ozdemir, A. Calik and A. Kokce, *Superlattice. Microst.* **49** (2011) 124.
29. N. Ucar, A.F. Ozdemir, D.A. Aldemir, S. Cakmak, A. Calik, H. Yildiz and F. Cimilli, *Superlattice. Microst.* **47** (2010) 586.
30. S. Sönmezoğlu, F. Bayansal and G. Çankaya, *Physica B* **405** (2010) 287.
31. G. Çankaya and B. Abay, *Semicond. Sci. Tech.* **21** (2006) 124.
32. K. Akkiliç, A. Türüt, G. Çankaya, T. Kiliçoğlu, *Solid State Commun.* **125** (2003) 551.
33. M. Çakar1, C. Temirci, A. Türüt and G Çankaya, *Physica Scripta* **68** (2003) 70.
34. G. Cankaya and N. Ucar, *Indian J. Pure Ap. Phys.* **41** (2003) 36.
35. G. Cankaya and N. Ucar, *Int. J. Electron.* **89** (2002) 745.
36. G. Cankaya and N. Ucar, *Physica Scripta* **65** (2002) 454.
37. C.S. Gworker, P. Phatak, B.T. Jonker, E.R. Weber and N. Newman, *Phys. Rev. B* **64** (2001) 045322.
38. E.M. Dizhur, A.Y. Shulman, I.N. Kotelnikov and A.N. Voronovsky, *Phys. Staus Solidi b* **223** (2001) 129.
39. G. Cankaya, N. Ucar and A. Turut, *Int. J. Electron.* **87** (2000) 1171.

40. G. Cancaya, N. Ucar and A. Türüt, *Phys. Status Solidi a* **179** (2000) 479.
41. G. Çankaya *et al.*, *Phys. Rev. B* **60** (1999) 15944.
42. P. Phatak, N. Newman, P. Dreszer and E.R. Weber, *Phys. Rev. B* **51** (1995) 18003.
43. M.J. Peanasky and H.G. Drickamer, *J. Appl. Phys.* **56** (1984) 3471.
44. O. Oubram, M.E. Mora-Ramos and L.M. Gaggero-Sager, *J. Phys. Conf. Ser.* **167** (2009) 1.
45. O. Oubram, M.E. Mora-Ramos and L.M. Gaggero-Sager, *Eur. Phys. J.B.* **71** (2009) 233.
46. F.J. Culchac, N. Porras-Montonegro and A Latgé, *J. Appl. Phys.* **105** (2009) 094324.
47. P.Y. Yu and M. Cardona, *Fundamentals of Semiconductors* 2nd ed., Springer, (Berlin 1999).
48. S.T. Pérez-Merchancano, R. Franco, J. Silva-Valencia, *Microelectron. J.* **39** (2008) 383.
49. M.G. Barseghyan, Alireza Hakimyard, S.Y. López, C.A. Duque and A.A. Kirokossyan, *Physica E* **42** (2010) 1618.
50. E. Kasapoglu, F. Ungan, H. Sari, I. Sökmen, *Physica E* **42** (2010) 1623.